

CO OXIDATION ON LaCoO_3 PEROVSKITE

Choong Kyun Rhee* and Ho-In Lee**

Dept. of Chem. Tech., College of Eng., Seoul National University, Seoul 151-742, Korea

(Received 31 August 1993 • accepted 26 October 1993)

Abstract—A study of CO oxidation on LaCoO_3 perovskite was performed in an ultrahigh vacuum system by means of adsorption and desorption. All gases were adsorbed at ambient temperature. Two adsorption states (α - and β -) of CO exist. The α -peak at 440 K is attributed to carbonyl species adsorbed on Co^{3+} ions while the β -peak at 663 K likely comes from bidentate carbonate formed by adsorption on lattice oxygens. CO_2 shows a single desorption peak (β -state, 483 K) whose chemical state may be monodentate carbonate. A new CO_2 desorption peak at 590 K can be created by oxidation of CO. O_2 also shows two adsorption states. One desorbs at 600 K, which may reflect adsorption on Co^{3+} ions. The other apparently incorporates with bulk LaCoO_3 and desorbs above 1000 K. The two adsorption states of CO are oxidized via different mechanisms. The rate determining step in oxidation of α -CO is the surface reaction whereas for that of β -CO, it is desorption of product CO_2 .

INTRODUCTION

The increased number of vehicles has induced air pollution and the problem has become more serious. Major pollutants in the exhaust gas are CO, NO_x and unburned hydrocarbons. The current policy for removal of these gases relies on the use of catalysts which are highly active for oxidation and reduction of the pollutants [1]. Noble metals like Pt, Pd and Rh are active but are very expensive due to their limited amount of deposit [2]. The need of catalysts based on more widespread and abundant elements is obvious. Some interesting results were obtained with perovskite type catalysts as a substitute for noble metal catalysts [3].

Cobaltate and manganate are active for oxidation of CO and reduction of NO [4, 5], but it is reported that the activities of perovskites are lower than that of Pt at low CO concentration [6, 7]. Perovskite type catalysts show high resistance against Pb derived from fuel because Pb can be a constituent of perovskite [8]. But severe deactivation by SO_2 dampened the initial enthusiasm for their application in automobile converters [9]. Such a deactivation can be reduced by doping noble metals into perovskite [10, 11].

The important catalytic properties of perovskite are

primarily the stability of valence states of metal ions, the mobility of lattice oxygen ions, and the stabilization of noble metals in high dispersion.

This study was performed in order to obtain the fundamental information about CO oxidation on perovskite type catalysts. LaCoO_3 perovskite was selected for its high activity and a UHV system was utilized to simplify the reaction system. AES and XPS were employed to obtain the cleanliness and stoichiometry of the surface and to identify the adsorption states of adsorbates. Also, TDS was used to distinguish the adsorption states and to elucidate the reaction mechanism.

EXPERIMENTAL

The stainless steel bell jar was evacuated by an ion pump, whose actual working pressure was $1-2 \times 10^{-9}$ Torr. Commercial AES/XPS (Perkin-Elmer, PHI 558) with CMA was employed. In XPS analyses, the Mg K_{α} X-ray photon (1253.6 eV) was used. Since the catalyst used in this experiment was an oxide, it showed charging effects by electron loss during photoemission. To remove the effect, an electron flood gun (EFG) was employed. The data acquisition in AES/XPS and the numerical calculation were performed by a PDP 11 computer with MACS system programmed by Perkin-Elmer.

The heating apparatus was specifically designed because the employed catalyst was powder. Tantalum

*Present address: Department of Chemistry, Chungnam National University, Taejeon 305-764, Korea

**To whom correspondences should be addressed.

foil was used for resistive heating. The foil was deformed into a basket shape, and a stainless steel net was spot-welded at the interior of the basket to hold the powder in place. A chromel-alumel thermocouple spot-welded to the bottom of the basket was calibrated with an optical pyrometer. The adsorption temperature and the heating rate during TDS were 300 K and 67 K/sec, respectively. The distance between the analyzing head of a quadrupole mass spectrometer and the catalyst was about 10 cm during the acquisition of TDS data. The amount of exposure was given in the unit of Langmuir (1L = 10⁻⁶ Torr·sec). AMU in figures is the abbreviation of atomic mass unit.

LaCoO₃ perovskite was prepared by coprecipitating [8, 12] a 1 : 1 mole ratio solution of La(NO₃)₃ (Yakuri, G.R.) and CO(NO₃)₂ (Yakuri, G.R.) with an (NH₄)₂CO₃ (Junsei, E.P.) solution. The coprecipitate of carbonates was separated by filtering and washed with cold water. After drying for 7 hours at 200°C, the precipitate was calcined at 900°C for 23 hours in a porcelain crucible. The powder was pressed at 300 kg/cm² into a plate which was heated to 1100°C for 5.5 hours. It was ground to powder and analyzed with an XRD (Rikagu, D-MAX-2A) whose target and filter were Cu and Ni, respectively. The well crystallized LaCoO₃ perovskite was obtained without any secondary phases. Its surface area determined by N₂ adsorption (B.E.T. method) was 0.808 m²/g assuming that the cross section of N₂ is 16.2 Å² [13].

Richter et al. [14] have reported a procedure to prepare a clean and stoichiometric surface of LaCoO₃, an indication of which is its single O (1s) peak with FWHM of 1.7 eV. Our perovskite had a somewhat broader peak than that of Richter et al. The surface potential of powder sample cannot be adjusted within ± 0.5 eV accuracy, even though an EFG is used [15]. The physical form of LaCoO₃ which Richter et al. used was a sintered material, but ours was the form of powder. Since a sharp peak with a FWHM of 1.7 eV could not be obtained in our experiment, the clean and stoichiometric surface of the powder LaCoO₃ was defined as that with a single O (1s) peak whose FWHM was 2.7 eV. This definition was very reproducible and maintained throughout the experiment. Even though LaCoO₃ had been made from carbonates, the content of surface carbon was below the detection limit in the AES spectrum.

The gas phase reagents used in this study were CO, CO₂, and O₂. All the gases were purchased from Nippon Sanso Company, and their quoted purities were 99.9% (CO), 99.9% (CO₂), and 99.99% (O₂), except liquid nitrogen trapping (in the case of CO₂, CO₂

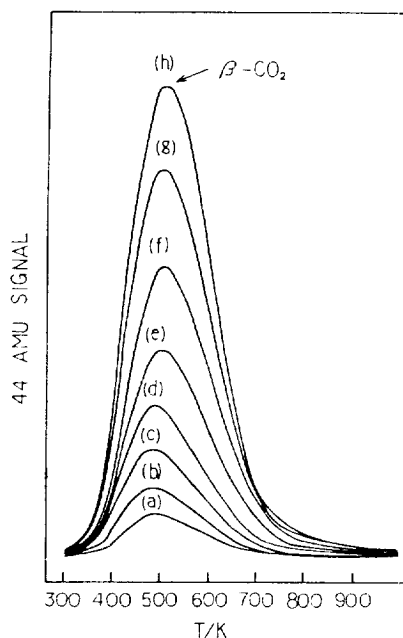


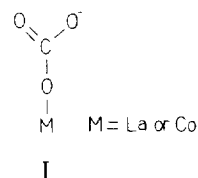
Fig. 1. Thermal desorption spectra of CO₂ after an exposure of (a) 2.2 L, (b) 4.2 L, (c) 8.5 L, (d) 17 L, (e) 34 L, (f) 68 L, (g) 127 L, and (h) 255 L.

itself was trapped), no more purification was given.

RESULTS AND DISCUSSION

1. CO₂ TDS

CO₂ TDS spectra are shown in Fig. 1. CO₂ adsorbed on LaCoO₃ shows a maximum desorption rate at 493 K and first-order desorption kinetics. Such a state of CO₂ is designated β-state. Model I is suggested as



an adsorption state of CO₂ on LaCoO₃ as reported previously [16]. CO₂ combines with a lattice oxygen to be monodentate carbonate. C (1s) peak of Model I is shown in Fig. 2. Background-correction was carried out in Fig. 2 because the base lines in the original spectra were not exactly horizontal. In most cases, the XPS peaks appear on a little background, which have to be removed by appropriate method for the purpose of the measurement of intensity [17]. The XPS C (1s) spectrum was obtained after a clean LaCoO₃

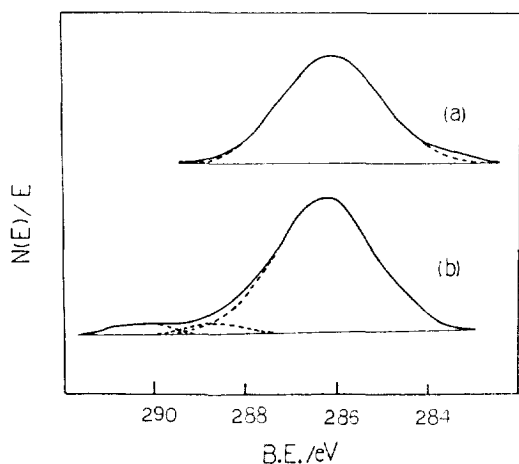


Fig. 2. (a) XPS C (1s) peak after a clean LaCoO_3 surface was exposed to 318 L of CO_2 , and (b) XPS C (1s) peak after a clean LaCoO_3 surface was exposed to 3840 L of CO. Both peaks were background-corrected and curve-fitted.

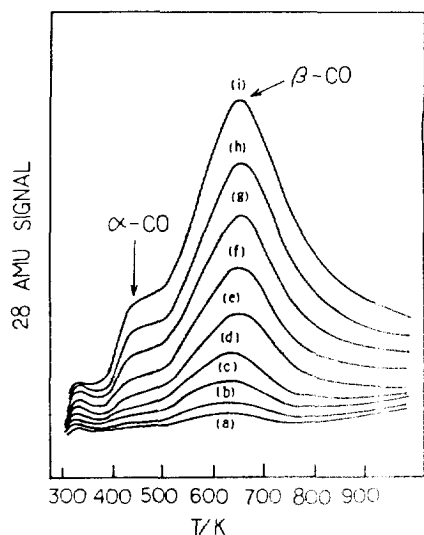


Fig. 3. Thermal desorption spectra of CO after an exposure of (a) 8 L, (b) 16 L, (c) 32 L, (d) 64 L, (e) 128 L, (f) 240 L, (g) 480 L, (h) 960 L, and (i) 1440 L.

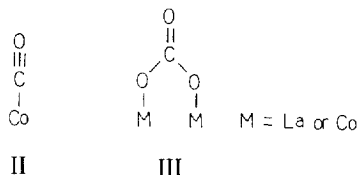
surface was exposed to 318 L of CO_2 . There is only one adsorption state on the CO_2 -exposed LaCoO_3 surface, whose binding energy is 286.0 eV.

2. CO TDS

Two adsorption states of CO on LaCoO_3 are shown in Fig. 3. One desorbs at 440 K, which is called α -state, and the other at 633 K, β -state. Each state has first-

order desorption kinetics. It was verified from a blank experiment that the desorption peak around 330 K originated from the blank.

Model II represents the bonding between Co^{3+} ion and adsorbed CO, which can be formed by electron back-donation. Such a carbonyl species has been suggested elsewhere [8, 18]. The desorption temperatures of CO from Co (1010) [19], Co (1012) [20] and Co (0001) [21] surfaces are 410, 440 and 420 K, respectively. These temperatures are similar to α -CO desorption temperature of our experiment. It is thought that no bond can be formed between La^{3+} and CO because of the filled orbitals in La^{3+} ion. Although the possibility of bridge-type CO bonds on Co^{3+} ions cannot be excluded, the distance between two Co^{3+} ions is about 4\AA [8], which is too far to form bridge-type species. Therefore, Model II is quite reasonable for the adsorption state of α -CO.



The β -state of CO on LaCoO_3 is suggested as Model III, where M is Co^{3+} and/or La^{3+} ions. This adsorption state of CO is thought to be a carbonate species as shown in IR results [22]. Two kinds of carbonate, monodentate and bidentate, are possible. If the adsorption state of β -CO is monodentate, two oxygens must be supplied from the surface. So the bridge-type CO bond with two lattice oxygens should be more easily formed. The population of β -CO seems to be lower than that of β - CO_2 , because each CO molecule must find two lattice oxygens with an appropriate distance to form a bidentate carbonate.

An XPS C (1s) spectrum was obtained after a clean LaCoO_3 surface was exposed to 3840 L of CO, as shown in Fig. 4. There are three peaks, whose binding energies are 286.2, 288.6 and 290.2 eV, respectively. The result was very reproducible. The peak of 286.2 eV is nearly consistent with that in Fig. 2, whose model is monodentate carbonate. The peaks of 288.6 and 290.2 eV correspond to carbonyl state and bidentate carbonate state, respectively. C (1s) electrons in Model I are more shielded by the valence electrons than those of carbon atom in Model III because of negative charge on Model I. Due to the direct bond to metal ion, the binding energy of C (1s) electrons in the carbonyl species is lower than that of the bidentate carbonate species. The existence of monodentate carbo-

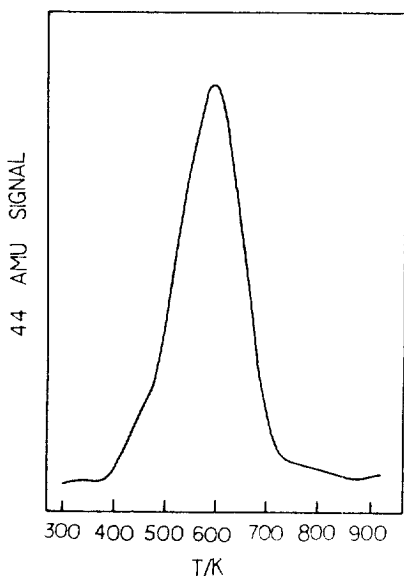


Fig. 4. Thermal desorption spectra of CO_2 after a clean LaCoO_3 surface was exposed to 100 L of CO only.

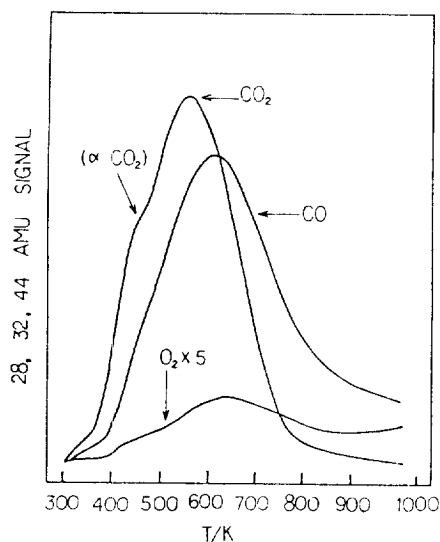


Fig. 6. Thermal desorption spectra of CO_2 , CO and O_2 after dosing 350 L of O_2 to the surface pre-exposed to 480 L of CO.

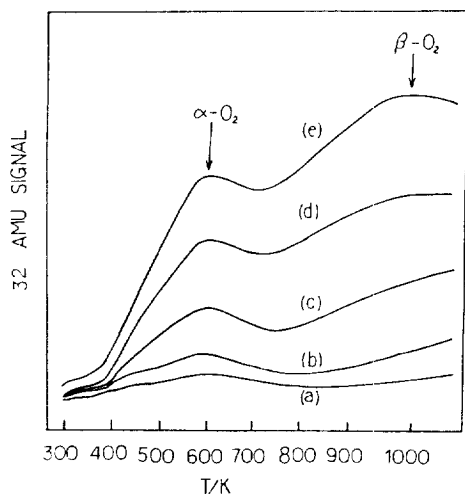


Fig. 5. Thermal desorption spectra of O_2 after an exposure of (a) 58 L, (b) 175 L, (c) 350 L, (d) 700 L, and (e) 1050 L.

nate on the CO-exposed LaCoO_3 surface may result from the transition of bidentate carbonate. In other words, the adsorbed CO reacts with lattice oxygen resulting in monodentate carbonate. The following experimental result supports the above discussion. The binding energy of C (1s) from the monodentate carbonate on the CO-exposed LaCoO_3 is always higher by about 0.2 eV than that of $\beta\text{-CO}_2$, suggesting that there

still exists, even if little, the character of bidentate carbonate as a result of precursor state during the transition.

A CO_2 TDS spectrum could be also obtained after a clean surface was exposed to CO only, as shown in Fig. 5. Such a fact is an evidence that adsorbed CO reacts with lattice oxygen, and most of all produced CO_2 are $\beta\text{-CO}_2$. So the monodentate carbonate desorbs as CO_2 only when heated in TDS, but the bidentate carbonate does as CO only. The reduction of perovskite by CO has been observed [16, 23].

3. O_2 TDS

O_2 TDS spectra are shown in Fig. 6. The α -state desorbs at 600 K and has first-order desorption kinetics. The β -state desorbs above 1000 K with second-order desorption kinetics.

Presumably, $\alpha\text{-O}_2$ exists on the surface, whose adsorption site would be oxygen vacancy or Co^{3+} ion [24, 25]. On the other hand, Nakamura et al. interpreted $\alpha\text{-O}_2$ as adsorbed or weakly-bound lattice oxygen [26]. Oxygen desorbing from the bulk may correspond to the β -state in O_2 TDS [24-26]. Adsorbed oxygen dissociates on the surface and penetrates into the bulk [23].

An O (1s) spectrum which is similar to the previous result [14] was obtained. Higher binding state corresponds to $\alpha\text{-O}_2$. The O (1s) peak of $\beta\text{-O}_2$ superimposes on that of lattice oxygen, suggesting that the oxygen incorporated into the bulk segregates to the surface

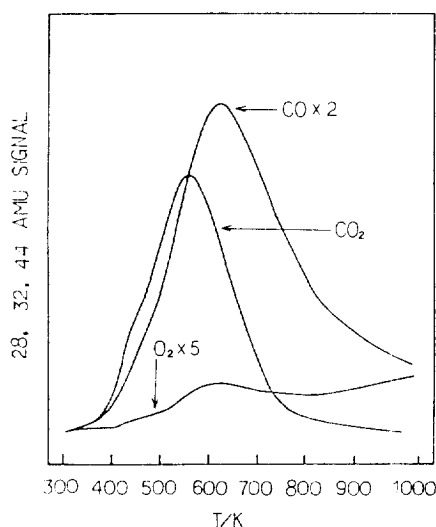


Fig. 7. Thermal desorption spectra of CO_2 , CO and O_2 after dosing 480 L of CO to the surface pre-exposed to 350 L of O_2 .

and desorbs as the substrate is heated. It is plausible that $\beta\text{-O}_2$ cannot be distinguished from the lattice oxygen.

4. Coadsorption of CO and O_2

Fig. 7 shows the TDS spectra of CO_2 , CO and O_2 , which were obtained after exposing a CO-covered surface to O_2 . The amounts of predosed CO and postdosed O_2 were 480 and 350 L, respectively. A new desorption peak of CO_2 is observed at the temperature of $\alpha\text{-CO}$ desorption, and the α -state of CO disappears mostly in the CO TDS spectrum. This new desorption state of CO_2 is designated α -state. The surface covered with 350 L O_2 was exposed to 480 L CO, and the TDS spectra of CO_2 , CO and O_2 were obtained as shown in Fig. 8. The α -state in the CO TDS spectrum disappears completely and a little $\alpha\text{-CO}_2$ is shown.

The disappearance of $\alpha\text{-CO}$ suggests the participation of $\alpha\text{-CO}$ in the oxidation. The desorption temperature of $\alpha\text{-CO}_2$ (Figs. 6 and 7) is still lower than that of $\beta\text{-CO}_2$ (Fig. 1) and is rather similar to that of $\alpha\text{-CO}$. $\alpha\text{-CO}_2$ did not exist on the surface which was exposed to CO_2 only. It is, therefore, reasonable to think that the state of $\alpha\text{-CO}_2$ is unstable. The above results indicate that the surface reaction step between $\alpha\text{-CO}$ and a certain oxygen species is slower than the desorption step of the unstable $\alpha\text{-CO}_2$. This suggests that the surface reaction is the rate-determining step in the oxidation of $\alpha\text{-CO}$.

$\beta\text{-CO}$ participates in the oxidation reaction, too. Bidentate carbonate ($\beta\text{-CO}$) turns to monodentate carbo-

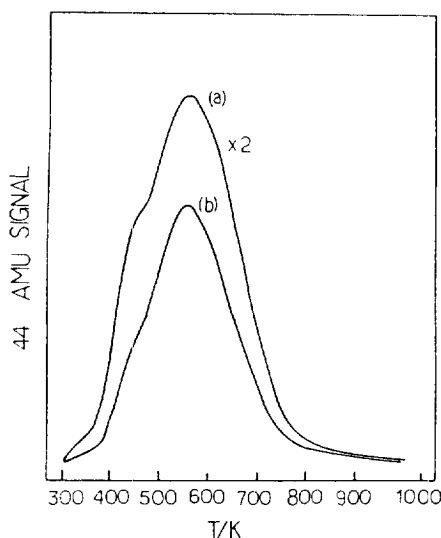


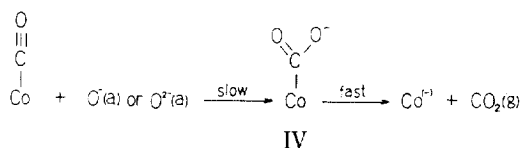
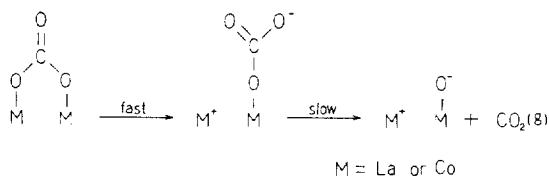
Fig. 8. Thermal desorption spectra of CO_2 (a) after dosing 350 L of O_2 to the surface pre-exposed to 480 L of CO, and (b) after dosing 480 L of CO to the surface pre-exposed to 350 L of O_2 .

nate ($\beta\text{-CO}_2$) and desorbs as a product of the reaction, CO_2 . The $\beta\text{-CO}_2$ produced by the oxidation of CO has a higher desorption temperature than the CO_2 desorbed from the CO_2 -exposed surface. This can also be explained in the same sense as discussed in Part 2 of this Section, that is, as a result of precursor state during the transition of $\beta\text{-CO}$. From this result, the desorption of the product may be the rate-determining step in $\beta\text{-CO}$ oxidation. As the concentration of $\alpha\text{-CO}$ is much lower than that of $\beta\text{-CO}$ as shown in Fig. 3, the overall oxidation is controlled by the $\beta\text{-CO}$ oxidation. The auto-inhibition of CO_2 in the CO oxidation on perovskite type catalysts [27, 28] supports the above discussion.

The intensity of $\beta\text{-CO}_2$ is higher in the case of O_2 -predosed surface than in that of O_2 -postdosed one, as shown in Fig. 9. This suggests that the preadsorbed oxygens act as adsorption sites of $\beta\text{-CO}$, which increases the concentration of bidentate carbonate.

The relatively higher intensity of $\alpha\text{-CO}_2$ in Fig. 8 than in Fig. 7 suggests that the adsorption sites of $\alpha\text{-CO}$ and of $\alpha\text{-O}_2$ are identical. In the case of preadsorption of O_2 , most of all Co^{3+} ions are blocked by the adsorbed oxygens. The blocked Co^{3+} ions are not available to the adsorption of $\alpha\text{-CO}$. On the other hand, in the case of preadsorption of CO, the population of $\alpha\text{-CO}$ is, therefore, so high to give more $\alpha\text{-CO}_2$.

The mechanisms of the $\alpha\text{-CO}$ and the $\beta\text{-CO}$ oxida-

Scheme 1. Oxidation of α -CO.Scheme 2. Oxidation of β -CO.

tions can be deduced from the results of this study. α -CO on Co^{3+} ion reacts slowly with adsorbed oxygen or lattice oxygen resulting in forming α -CO₂. The formed α -CO₂ desorbs readily for its unstability on the surface of LaCoO₃. The reaction mechanism of the α -CO oxidation is suggested as shown in Scheme 1. The β -CO, which adsorbs on lattice oxygen or adsorbed oxygen as a bridge-type for a bidentate, turns readily to a monodentate. And then, the formed monodentate carbonate desorbs slowly to gaseous CO₂. The suggested reaction mechanism of the β -CO oxidation is shown in Scheme 2.

CONCLUSIONS

1. Two adsorption states of CO exist on the surface of LaCoO₃. The desorption peak at 440 K is from carbonyl species adsorbed on Co^{3+} ion and that of 633 K, bidentate carbonate formed by adsorbing on lattice oxygen and/or adsorbed oxygen.

2. CO₂ shows a single desorption peak whose chemical state is monodentate carbonate. A new adsorption state of CO₂ is formed during the oxidation of CO on the surface.

3. O₂ shows two adsorption states. The one desorbs at 600 K, which adsorbs on Co^{3+} ion, and the other incorporates with the bulk of LaCoO₃ and desorbs above 1000 K.

4. Two adsorption states of CO are oxidized via different mechanisms. The rate-determining step in α -CO oxidation is surface reaction whereas that in β -CO oxidation, desorption of the product CO₂.

ACKNOWLEDGEMENT

The authors gratefully acknowledge the financial

support by the Korea Science and Engineering Foundation for this work.

REFERENCES

1. Shelef, M.: *Catal. Rev.*, **11**, 1 (1975).
2. Egelhoff, W. F., Jr.: "The Chemical Physics of Solid Surfaces and Heterogeneous Catalysis", Vol. 4, Eds. King, D. A. and Woodruff, D. P., Elsevier Scientific, New York, p. 424 (1982).
3. Libby, W. F.: *Science*, **171**, 499 (1971); Pedersen, L. A. and Libby, W. F.: *Science*, **176**, 1355 (1972).
4. Voorhoeve, R. J. H., Remeika, J. P., Freeland, P. E. and Mattias, B. T.: *Science*, **177**, 353 (1972).
5. Voorhoeve, R. J. H., Remeika, J. P. and Johnson, D. W., Jr.: *Science*, **180**, 62 (1973).
6. Schlatter, J. C., Klimisch, R. L. and Taylor, K. C.: *Science*, **179**, 798 (1973).
7. Yao, Y. F. Y.: *J. Catal.*, **36**, 266 (1975).
8. Voorhoeve, R. J. H., Johnson, D. W., Jr., Remeika, J. P. and Gallagher, P. K.: *Science*, **195**, 827 (1977).
9. Gallagher, P. K., Johnson, D. W., Jr., Vogel, E. M. and Schrey, F.: *Mater. Res. Bull.*, **10**, 623 (1975).
10. Gallagher, P. K., Johnson, D. W., Jr., Remeika, J. P., Schrey, F., Trimble, L. E., Vogel, E. M. and Voorhoeve, R. J. H.: *Mater. Res. Bull.*, **10**, 529 (1975).
11. Lauder, A.: *Chem. Eng. News*, **53**, 8 (1975).
12. Johnson, D. W., Jr., Gallagher, P. K., Schrey, F. and Rhodes, W. W.: *Ceramic Bull.*, **55**, 520 (1976).
13. Gregg, S. J. and Sing, K. S. W.: "Adsorption, Surface Area and Porosity", 2nd ed., Academic Press, New York, p. 62 (1982).
14. Richter, L., Bader, S. D. and Brodsky, M. B.: *Phys. Rev. B*, **22**, 3059 (1980).
15. Crespin, M. and Hall, W. K.: *J. Catal.*, **69**, 359 (1981).
16. Tascon, J. M. D. and Tejuca, L. G.: *J. Chem. Soc., Faraday Trans. 1*, **77**, 591 (1981).
17. Seah, M. P.: "Practical Surface Analysis", Eds. Briggs, D. and Seah, M. P., John Wiley & Sons, Ltd., New York, p. 203 (1983).
18. Kojima, I., Adachi, H. and Yasumori, I.: *Surface Sci.*, **130**, 50 (1983).
19. Habenschaden, E. and Küppers, J.: *Surface Sci.*, **138**, L147 (1984).
20. Prior, K. A., Schwaha, K. and Lambert, R. M.: *Surface Sci.*, **77**, 193 (1978).
21. Bridge, M. E., Comrie, L. M. and Lambert, R. M.: *J. Catal.*, **58**, 28 (1979).
22. Tascon, J. M. D. and Tejuca, L. G.: *Z. Phys. Chem. (N.F.)*, **121**, 63 (1980).
23. Tascon, J. M. D. and Tejuca, L. G.: *Z. Phys. Chem.*

- (*N.F.*), **121**, 79 (1980).
24. Yamazoe, N., Teraoka, Y. and Seiyama, T.: *Chem. Lett.*, 1767(1981).
25. Teraoka, Y., Zhang, H. M. and Yamazoe, N.: *Chem. Lett.*, 1367(1985).
26. Nakamura, T., Misono, M. and Yoneda, Y.: *Chem. Lett.*, 1589(1981).
27. George, S., Viswanathan, B. and Sastri, M. V. C.: *Ind. J. Chem.*, **15A**, 285(1977).
28. George, S. and Viswanathan, B.: *J. Colloid and Interface Sci.*, **95**, 322 (1983).
26. Nakamura, T., Misono, M. and Yoneda, Y.: *Chem.*